

## Supporting Information

### Calcination Activation of Three-dimensional Cobalt Organic

### Phosphate Nanoflake Assemblies for Supercapacitors

*Qingling Jing, Wenting Li, \* Jiajing Wang, Xudong Chen, Huan Pang\**

School of Chemistry and Chemical Engineering, Institute for Innovative Materials and Energy, Yangzhou University, Yangzhou, 225002, Jiangsu, P. R. China.

E-mail: huanpangchem@hotmail.com, panghuan@yzu.edu.cn (H. Pang)

wentinglichem@hotmail.com (W. Li)

#### 1 Experimental section

##### 1.1 Materials

All the chemicals in this study, including cobalt acetylacetonate( II ) methanol ( $\text{CH}_3\text{OH}$ ), Nickel foam, were used as received without further purification. All aqueous solutions were freshly prepared with high purity water ( $18\text{ M}\Omega\text{ cm}^{-1}$ ).

##### 1.2 Materials synthesis

##### Synthesis of COP precursors with different thickness.

$\text{C}_{10}\text{H}_{14}\text{CoO}_4$  (0.2 mmol) and  $\text{C}_6\text{H}_7\text{O}_3\text{P}$  (0.2 mmol) were dissolved in 5 ml methanol and stirred at room temperature for 4 h. Then the product was separated by centrifugation. Finally, the obtained samples were washed using deionized water and methanol to remove impurities and dried in air naturally, which obtained M1, M2, and M3 were synthesized as described above, halving  $\text{C}_{10}\text{H}_{14}\text{CoO}_4$  and  $\text{C}_6\text{H}_7\text{O}_3\text{P}$  from 0.2 mmol to 0.1 mmol and 0.05 mmol and keeping the volume of methanol unchanged.

##### Preparation of COP assemblies

Among the COP precursors synthesized above, the samples with uniform nanoflake were selected and calcined in air at 100, 200, 300 and 400 °C. The heating rate was

maintained at 1 °C min<sup>-1</sup>, then the reaction stopped and the temperature decreased naturally, the obtained product noted as Mx-y (where x refers to reactant concentrations and y refers to activation temperatures).

### **1.3 Material characterization**

The morphological features were characterized by scanning electron microscopy (SEM, Zeiss-Supra 55), high resolution transmission electron microscopy (HRTEM, Tecnai G2 F30S-TWIN) and energy dispersive spectroscopy (EDS) mapping. X-ray diffraction (XRD) patterns were examined on a Bruker D8 Advanced X-ray diffractometer (CuK $\alpha$  radiation:  $\lambda$  = 0.15406 nm). The chemical states were analyzed using X-ray photoelectron spectroscopy (XPS) with monochromatic AlK $\alpha$  excitation under vacuum higher than  $1 \times 10^{-7}$  Pa. In addition, Fourier transform-Infrared Radiation (FT-IR) measurement was performed on BRUKER-EQUINOX-55 IR spectrophotometer. The thermogravimetric analysis (TGA) was performed under air atmosphere with a heating rate of 10 °C min<sup>-1</sup> by using a Pyris 1 TGA thermogravimetric analyzer. All electrochemical measurements were carried out by using a CHI 660E instrument.

### **1.4 Electrochemical measurements**

The electrochemical measurements were carried out with CHI660e working station in 3.0 M KOH solution at room temperature. Galvanostatic charge-discharge (GCD), Cyclic voltammetry (CV) and electrochemical impedance spectroscopy (EIS) methods were used to investigate the capacitive properties of the COP precursors and COP assemblies electrodes. The EIS measurements were conducted in the frequency range of 100 kHz to 0.01 Hz at the open-circuit voltage.

For the three-electrode cell, the working electrode was made by mixing the active materials (COP precursors and COP assemblies), acetylene black, and polytetrafluoroethylene at a weight ratio of 80: 15: 5. The slurry was coated on a piece of foamed nickel foam ( $\approx 1$  cm<sup>2</sup>), which was then pressed into a thin foil at a pressure of 10 MPa. The typical mass loading of the electrode material was 1.0 mg. A platinum electrode and a Hg/HgO electrode served as the counter and reference electrode, respectively.

When assembling an aqueous device, the active material (M3-200) was employed as positive electrode while negative electrode was activated carbon. The positive and negative electrodes were made by mixing active materials (M3-200)/activated carbon, acetylene black and polytetrafluoroethylene at a weight ratio of 80: 15: 5. The slurry was coated on a piece of foamed nickel foam ( $\approx 1 \text{ cm}^2$ ), which was then pressed into a thin foil at a pressure of 10 MPa. Generally, the charges stored by positive and negative electrodes can be determined by formula (1), where  $C_+$ ,  $C_-$  represent the specific capacitance of positive electrode and negative electrodes ( $\text{F g}^{-1}$ ), respectively;  $\Delta E$  is the potential range (V);  $m_+$ ,  $m_-$  is the weight of the active material in positive electrode and negative electrode (g), respectively; The charges are balanced by the equation of  $q_+ = q_-$ , where  $q_+$  and  $q_-$  represent the charges stored in the positive and negative electrodes, respectively. Therefore,  $m_+/m_- = C_- \times \Delta E_- / C_+ \times \Delta E_+$ .  $q_+ = C_+ \times \Delta E_+ \times m_+$  and  $q_- = C_- \times \Delta E_- \times m_-$ . (1)

### 1.5 Calculation

The specific capacitance of the electrode material can be calculated from the charge-discharge curves according to the equation:

$$C = Q / (m \times \Delta V) = \int I dt / (m \times \Delta V) = I \times t_{\text{discharge}} / (m \times \Delta V) \quad (2)$$

Where  $C$  is specific capacitance in  $\text{F g}^{-1}$ ,  $\Delta t$  is the discharging time in s,  $\Delta V$  is the potential window in V.

## 2 Supplementary data section

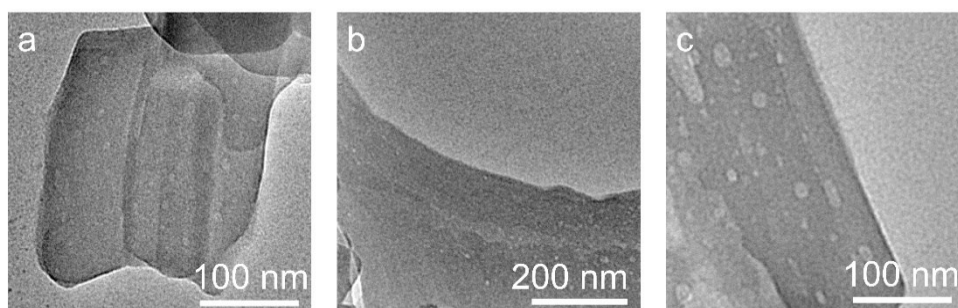


**Figure S1.** TEM images of a) M1; b) M2; c) M300.

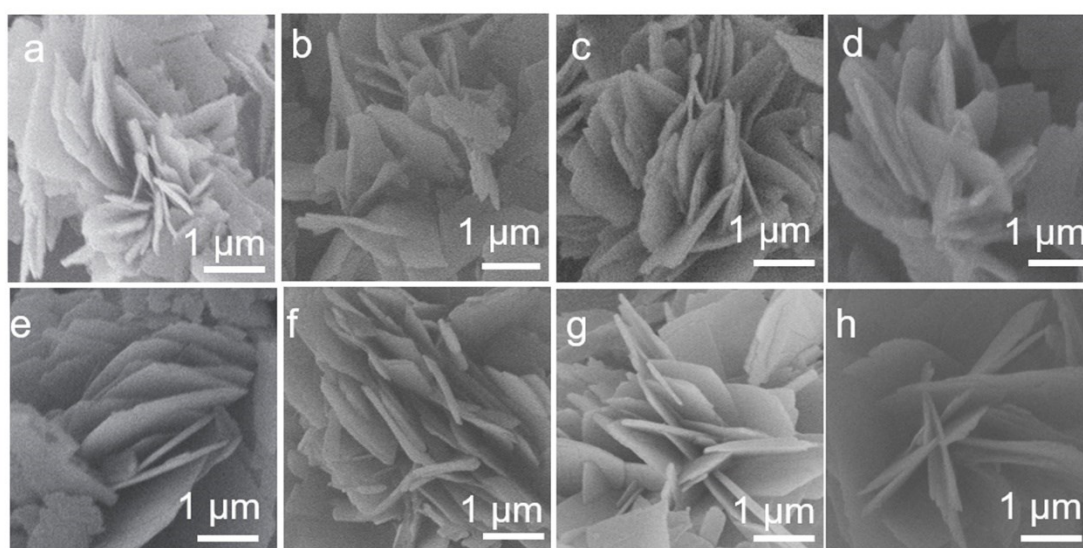


**Figure S2.** SEM images of a) M1-100; b) M1-200; c) M1-300; d) M1-400; e) M2-100; f) M2-200; g) M2-300; h) M2-400.

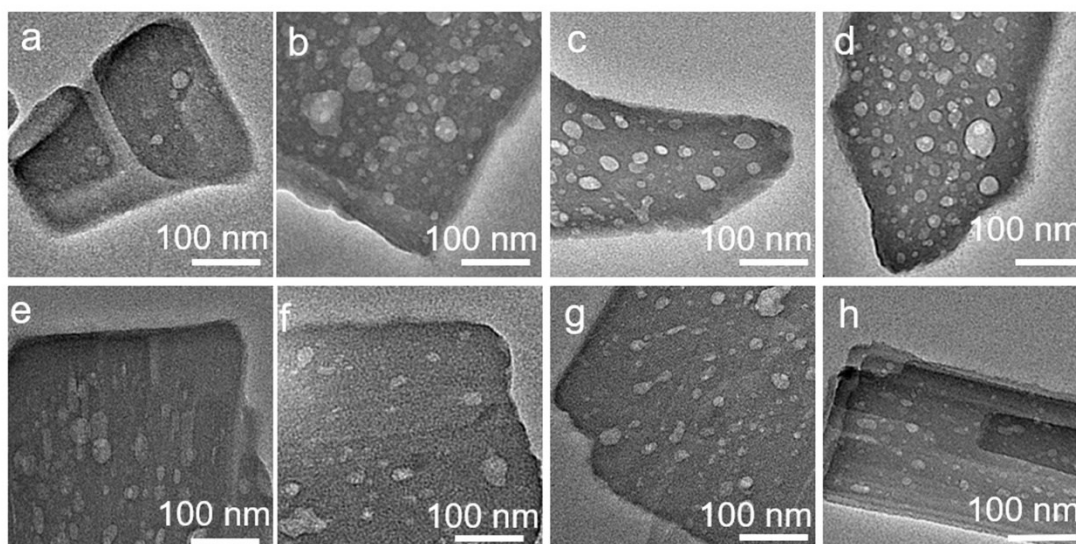


**Figure S3.** TEM images of a) M1-100; b) M1-200; c) M1-300; d) M1-400; e) M2-100; f) M2-200; g) M2-300; h) M2-400.

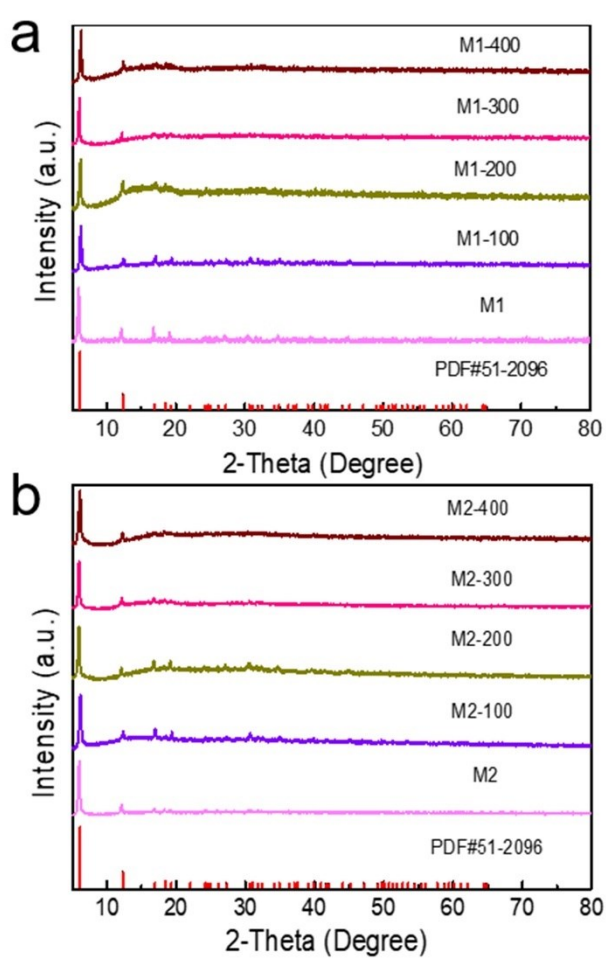


**Figure S4.** Experimental XRD patterns of a) M1, M1-100, M1-200, M1-300, and M1-400; b) M2, M2-100, M2-200, M2-300, and M2-400.

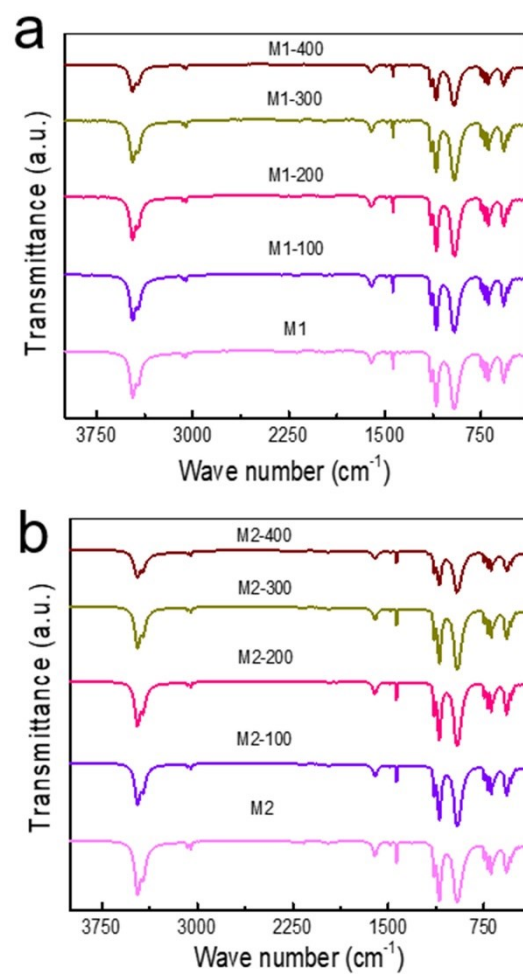


**Figure S5.** FT-IR spectra of a) M1, M1-100, M1-200, M1-300 and M1-400; b) M2, M2-100, M2-200, M2-300, and M2-400.

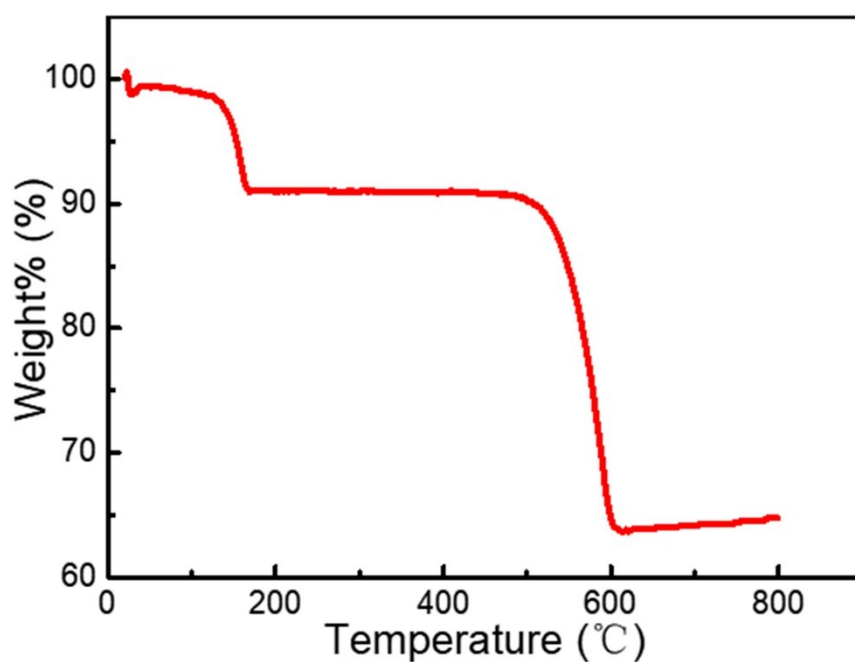


**Figure S6.** TG curves of M3.

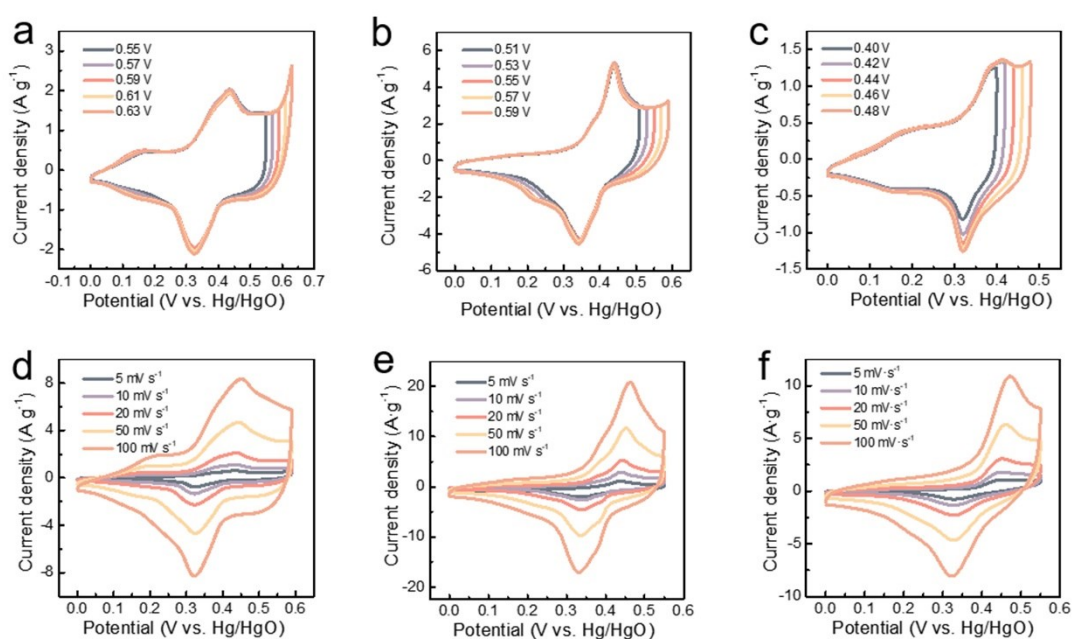


**Figure S7.** The CV curves with a scan rate at  $20 \text{ mV s}^{-1}$  of active materials in a three-electrode cell in  $3.0 \text{ M KOH}$  aqueous solution at different potentials: a) M1, b) M2, c) M3; The CV curves of active materials in a three-electrode cell in  $3.0 \text{ M KOH}$  aqueous solution at different scan rates: d) M1, e) M2, f) M3.

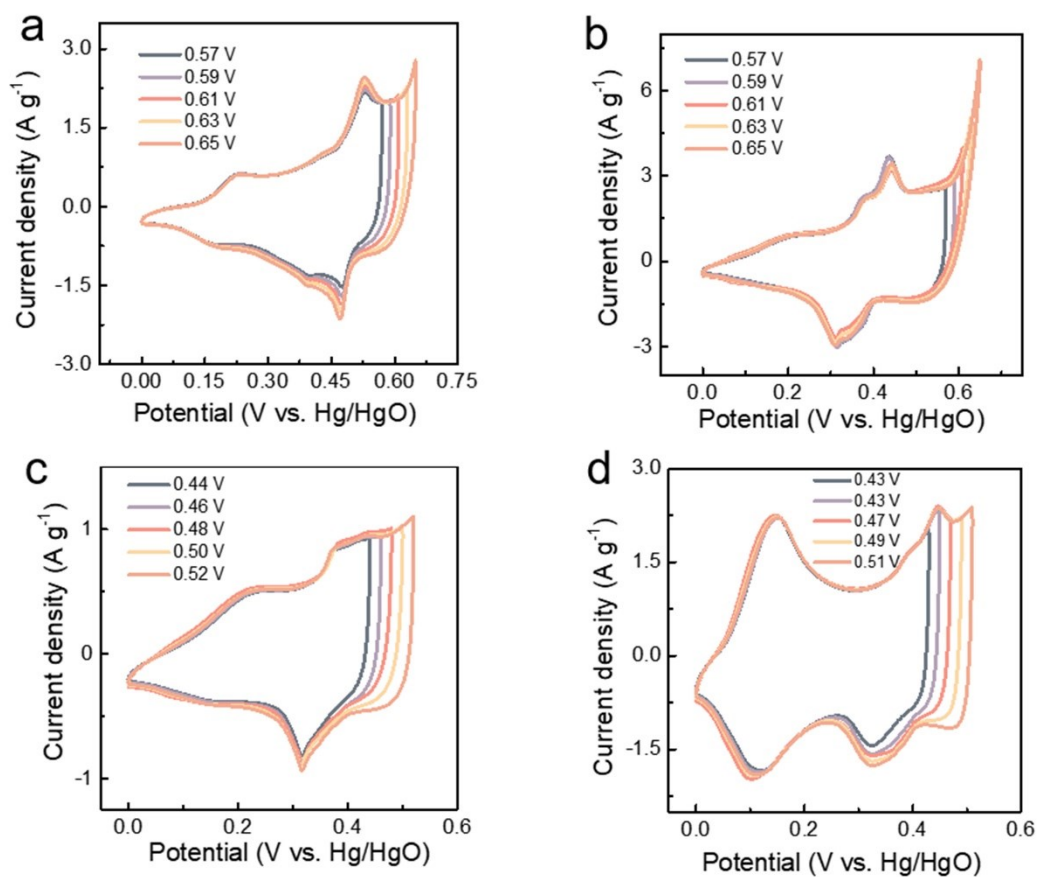


**Figure S8.** The CV curves with a scan rate at  $20 \text{ mV s}^{-1}$  of active materials in a three-electrode cell in  $3.0 \text{ M KOH}$  aqueous solution at different potentials: a) M1-100, b) M1-200, c) M1-300, d) M1-400.



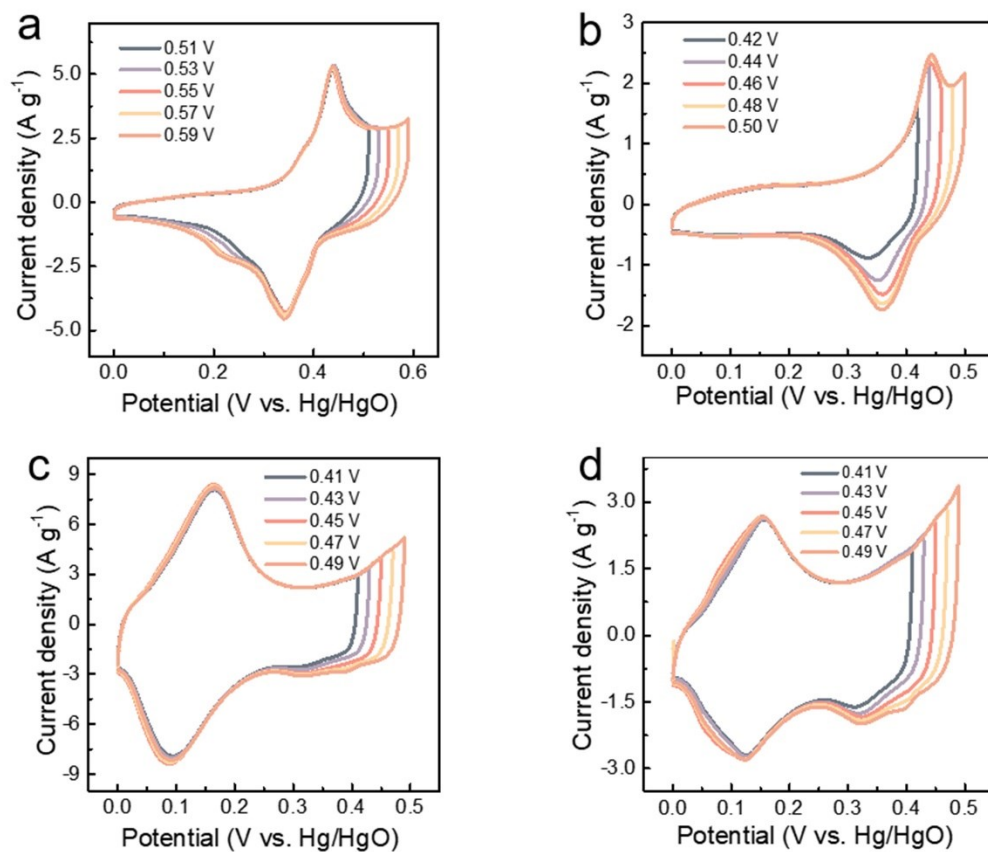


**Figure S9.** The CV curves with a scan rate at  $20 \text{ mV s}^{-1}$  of active materials in a three-electrode cell in  $3.0 \text{ M KOH}$  aqueous solution at different potentials: a) M2-100, b) M2-200, c) M2-300, d) M2-400.

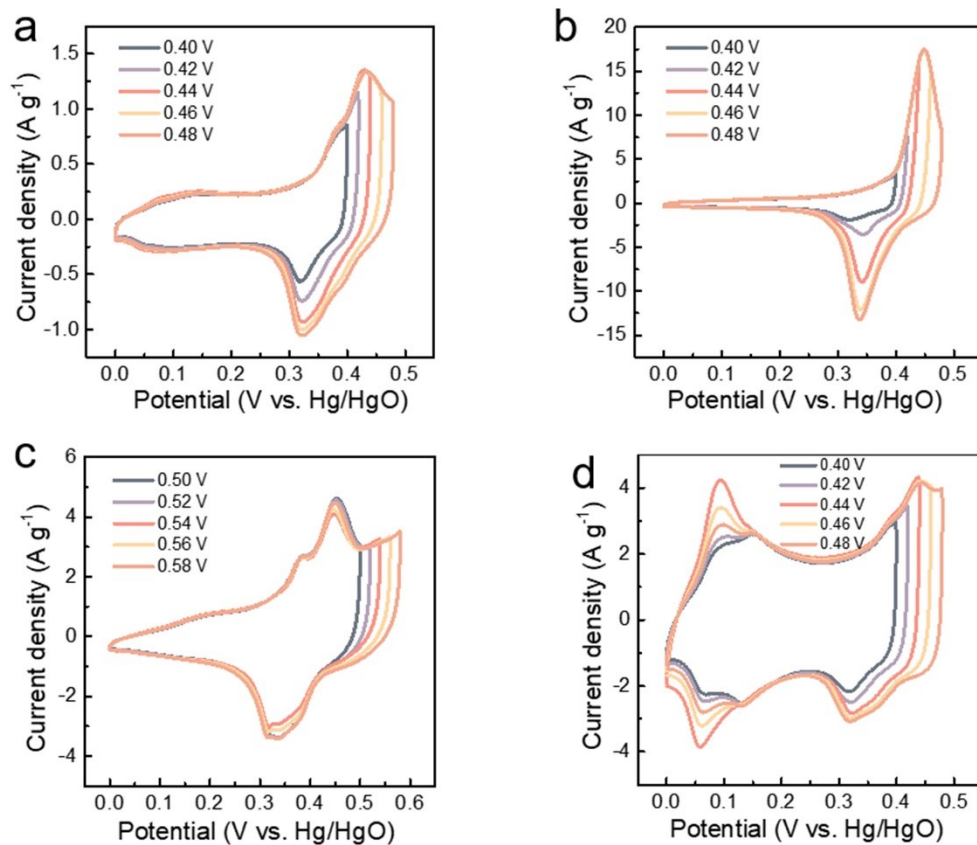


**Figure S10.** The CV curves with a scan rate at  $20 \text{ mV s}^{-1}$  of active materials in a three-electrode cell in 3.0 M KOH aqueous solution at different potentials: a) M3-100, b) M3-200, c) M3-300, d) M3-400.

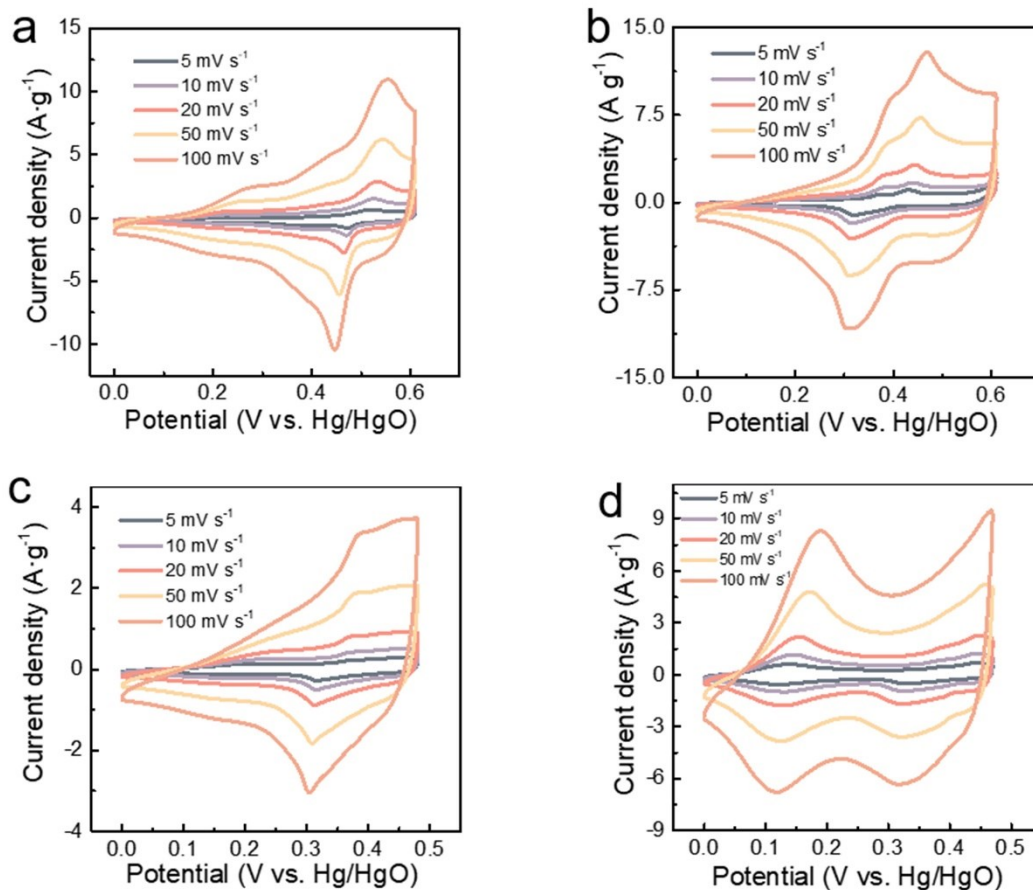


**Figure S11.** The CV curves of active materials in a three-electrode cell in 3.0 M KOH aqueous solution at different scan rates: a) M1-100, b) M1-200, c) M1-300, d) M1-400.

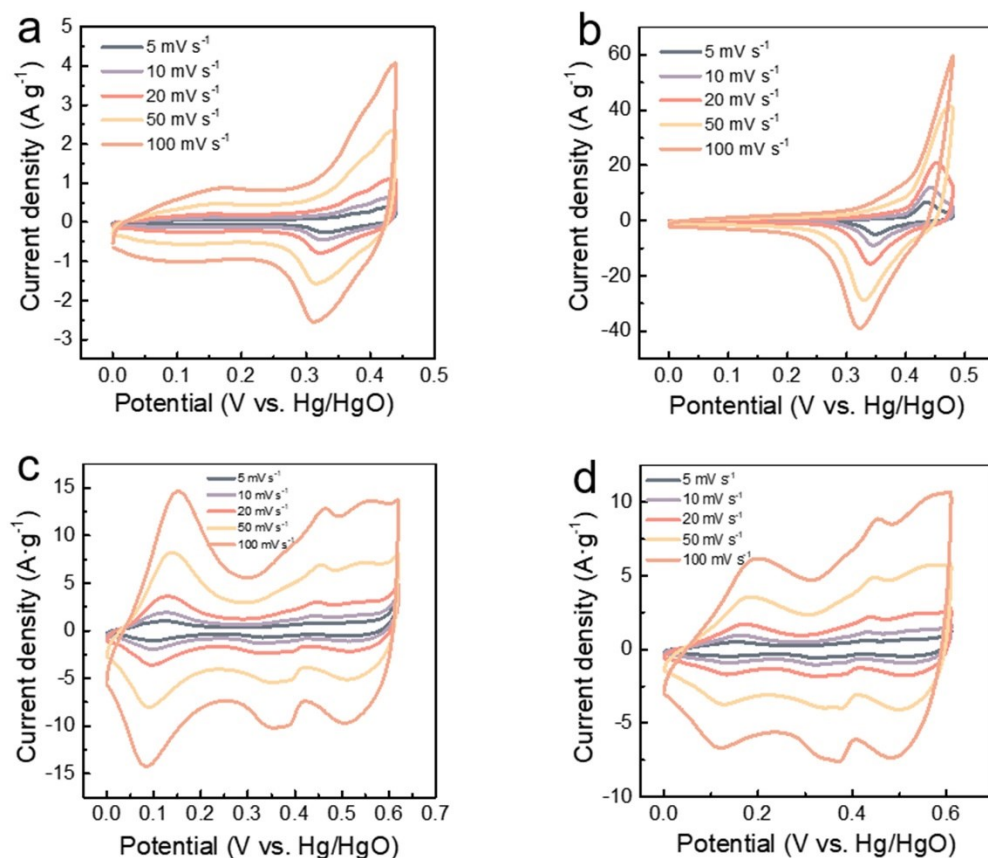


**Figure S12.** The CV curves of active materials in a three-electrode cell in 3.0 M KOH aqueous solution at different scan rates: a) M2-100, b) M2-200, c) M2-300, d) M2-400.

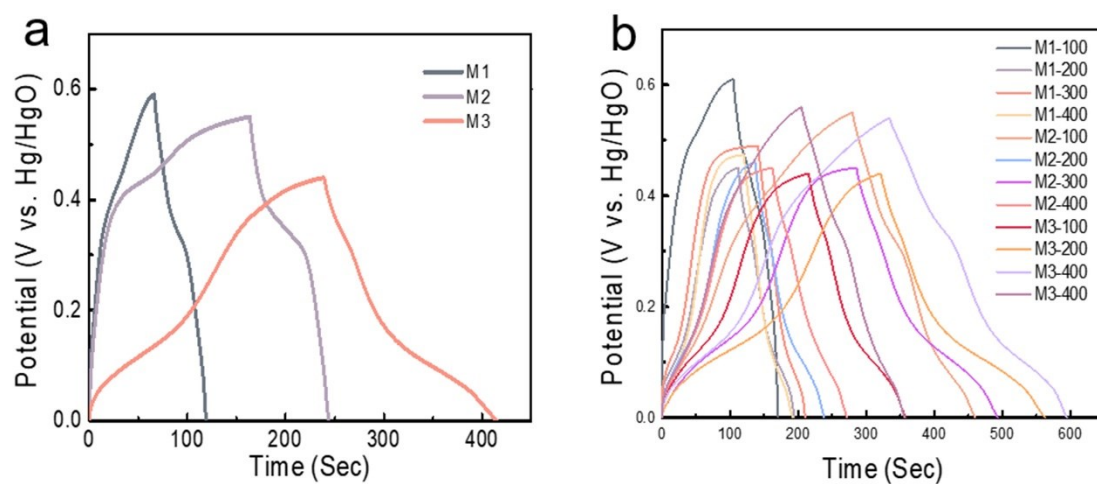


**Figure S13.** The CV curves of active materials in a three-electrode cell in 3.0 M KOH aqueous solution at different scan rates: a) M3-100, b) M3-200, c) M3-300, d) M3-400.

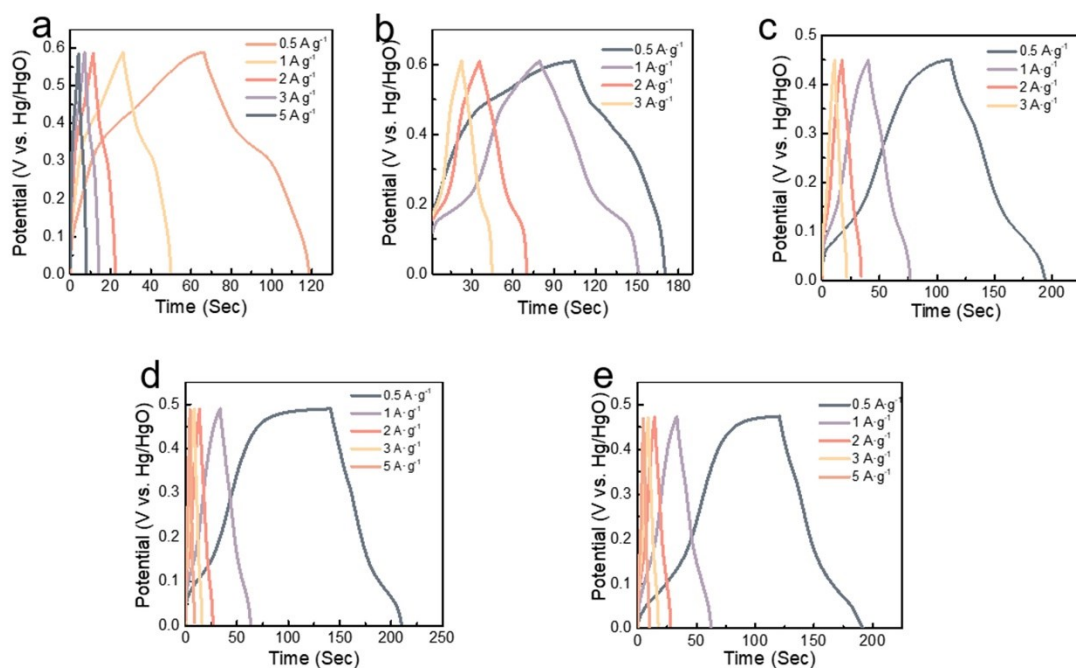


**Figure S14.** The GCD curves of active materials in a three-electrode cell in 3.0 M KOH aqueous solution at different current densities: a) M1, b) M1-100, c) M1-200, d) M1-300, e) M1-400.

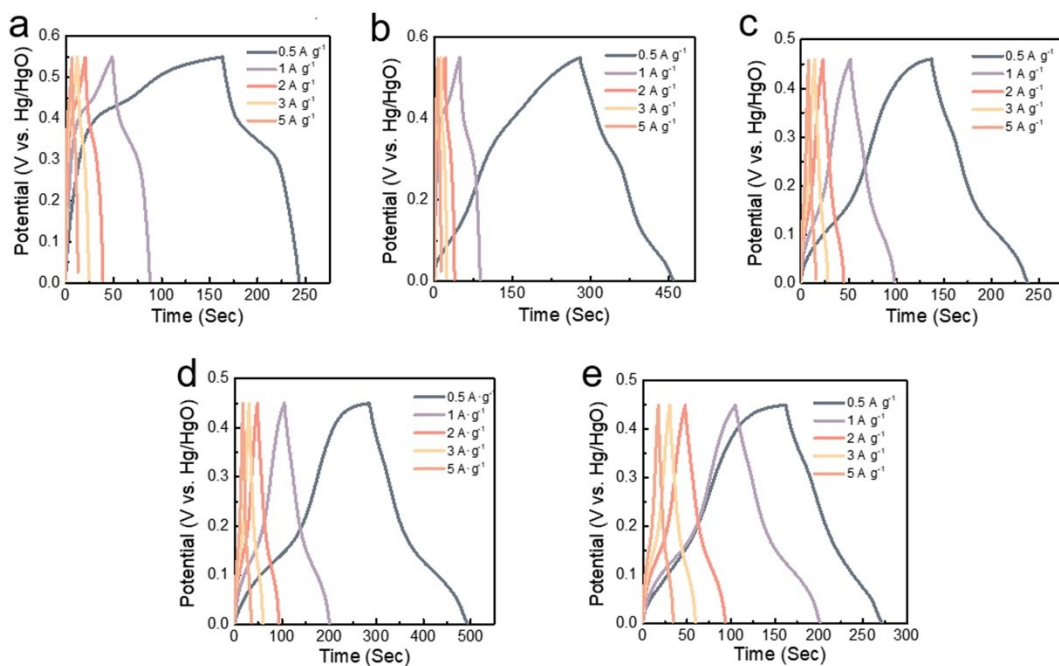


**Figure S15.** The GCD curves of active materials in a three-electrode cell in 3.0 M KOH aqueous solution at different current densities: a) M2, b) M2-100, c) M2-200, d) M2-300, e) M2-400.



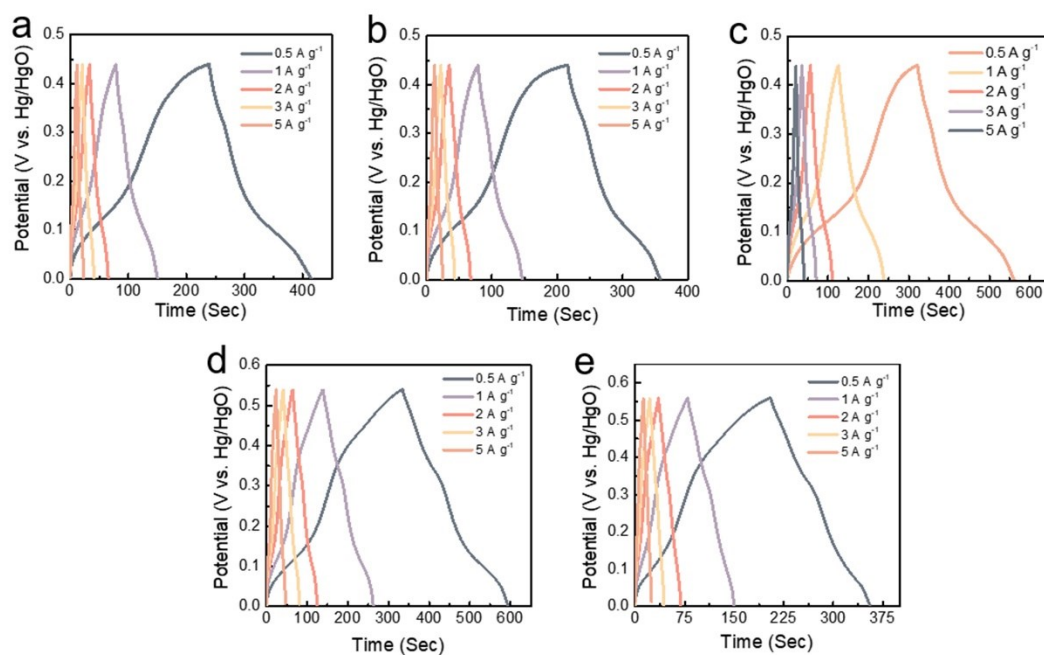


**Figure S16.** The GCD curves of active materials in a three-electrode cell in 3.0 M KOH aqueous solution at different current densities: a) M3, b) M3-100, c) M3-200, d) M3-300, e) M3-400.

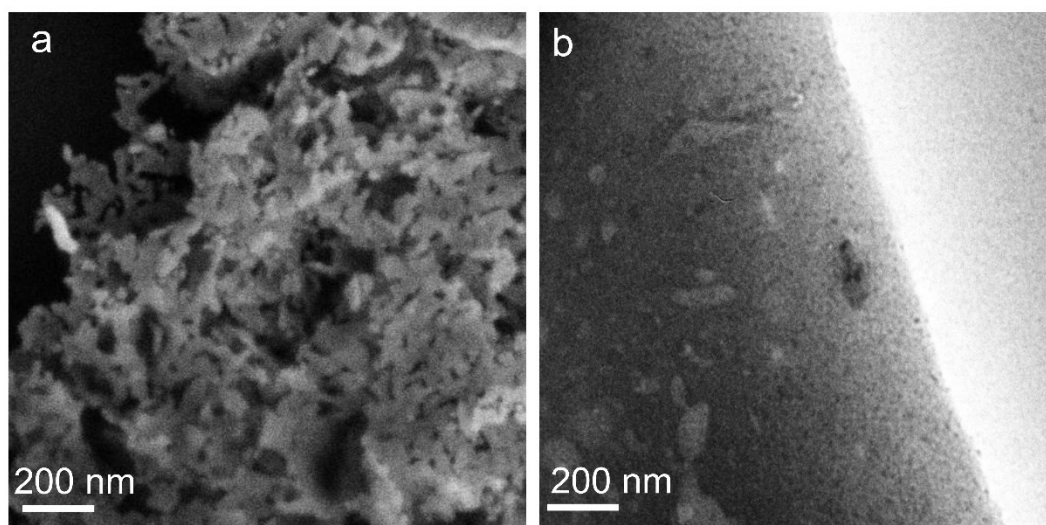


**Figure S17.** a) SEM image of M3-200 electrodes after long cycles; b) TEM image of M3-200 electrodes after long cycles.

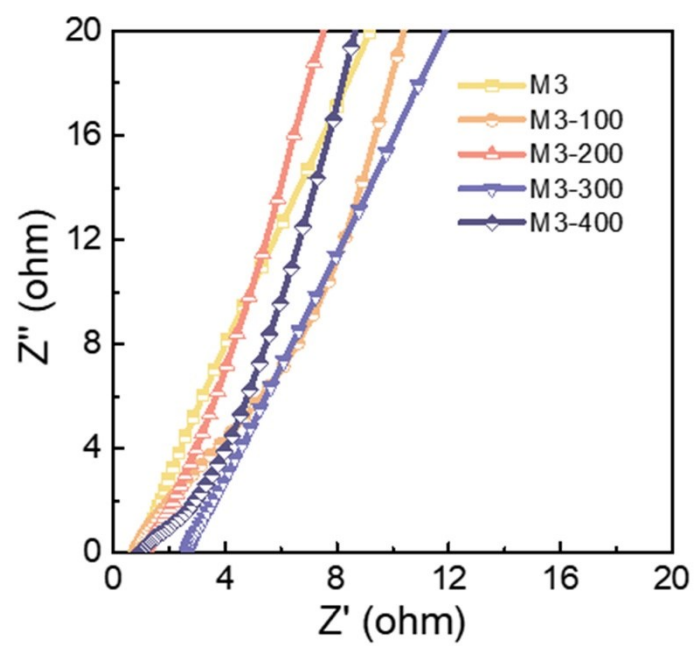


**Figure S18.** The EIS of the active materials in a three-electrode cell in 3.0 M KOH aqueous solution at room temperature.